A Kit Mutation Associated with Black-Eyed White Phenotype in the Grey Red-Backed Vole, Myodes rufocanus

Authors: Murakami, Shota, Tsuchiya, Kimiyuki, Nakata, Keisuke, Nishikata, Mana, Kitada, Kazuhiro, et al.

Source: Mammal Study, 47(4) : 235-247

Published By: Mammal Society of Japan

URL: https://doi.org/10.3106/ms2022-0003

Mammal Study 47: 235–247 (2022) DOI: 10.3106/ms2022-0003

Original paper

A *Kit* mutation associated with black-eyed white phenotype in the grey red-backed vole, *Myodes rufocanus*

Shota Murakami[1,*,], Kimiyuki Tsuchiya[2], Keisuke Nakata[3], Mana Nishikata[4], Kazuhiro Kitada[4] and Hitoshi Suzuki[1]**

[1] *Graduate School of Environmental Science, Hokkaido University, Sapporo, Hokkaido, Japan*
[2] *Laboratory of Bioresources, Applied Biology Co. Ltd, Minato-ku, Tokyo, Japan*
[3] *Forestry Research Institute, Hokkaido Research Organization, Bibai, Hokkaido, Japan*
[4] *Graduate School of Life Science, Hokkaido University, Sapporo, Hokkaido, Japan*

Abstract. Mutations in genes causing leucism are often accompanied by serious disease limiting individual fitness in laboratory animals. Mammalian species with all-white fur exist in the wild; however, the causative genes have not yet been identified, because of the difficulty of the forward genetic approach—comparisons between individuals with different phenotypes. In this study, we conducted linkage analyses using six candidate gene markers on a wild leucistic female grey red-backed vole (*Myodes rufocanus*) and inbreeding F1 and F2 offspring displaying variations in coat colors, agouti, and leucism. We found that the white-furred variant was associated with a specific *Kit* allele characterized by a nonsynonymous substitution at amino acid position 604, leading to the replacement of glycine with arginine. In addition, the leucistic phenotype was accompanied by a small portion of black hairs, which increased with growth. Our results showed a candidate gene causing leucism in viable wild animals and provided an opportunity to consider the necessity to study growth-associated traits for coat color analyses.

Key words: coat color, growth-associated trait, *Kit*, leucism, *Myodes rufocanus*.

Coloration in mammals is thought to have ecologically and evolutionarily important functions, including concealment, thermoregulation, and signaling (Caro 2005; Caro and Mallarino 2020). For instance, white coat colors are found in Arctic tundra habitats (Caro 2005). Camouflage has long been thought as the strongest evolutionary force on white coat coloration, making individuals less visible to their predators and prey in snowy environments (Wallace 1877; Cott 1940; Zimova et al. 2018). Several studies have also identified flashing behavior; for example, *Lepus* hares displaying a whitish ear with black hairs flash conspicuous coloration by moving their ears up and down, helping them escape from confused predators (Kamler and Ballard 2006; Kamler 2008; Caro and Mallarino 2020). Consequently, white coat coloration is an important trait for individuals to survive and colonize, especially in Arctic regions, by escaping predation and increasing their foraging efficiency.

White coat color phenotypes are classified into albinism and leucism. Albinism is defined by complete loss of pigmentation in hair, skin, and eyes (Fox and Vevers 1960; van Grouw 2006, 2013), as well as inner ear and retinal pigment epithelium (Motohashi et al. 1994; Shibuya et al. 2018), while leucism is defined by partial loss of pigmentation in the regions, varying in degree from partial to complete leucism (Fox and Vevers 1960; van Grouw 2006, 2013). For example, a phenotype with pigmented eyes and white hair on the entire body is called black-eyed white (Little 1915), which is a common leucistic phenotype in wild mammal species and populations such as the mountain goat, *Oreamnos americanus*; the polar bear, *Ursus maritimus*; and the northern population of the Arctic hare, *Lepus arcticus* (Cott 1940; Best and Henry 1994).

**To whom correspondence should be addressed. E-mail: shota-m@g.ecc.u-tokyo.ac.jp*
***Present address: Department of General Systems Studies, Graduate School of Arts and Sciences, The University of Tokyo, Meguro-ku, Tokyo, Japan*

More than 650 genes have been identified in human, mouse, and zebrafish to determine coat colors (Baxter et al. 2019), which are also affected by growth factors (Caro and Mallarino 2020). Mutations in genes such as *Kit* regulating the development of pigment-producing cells, melanocytes, during neural crest induction and differentiation cause not only leucistic phenotypes due to a lack of melanocytes in skin and hair follicles but also often disorders of sensory organs and reproduction via pleiotropic effects (Cieslak et al. 2011; Reissmann and Ludwig 2013). In particular, mutations in both *Kit* and *Kit ligand* (*Kitl*) genes, which are related to the proliferation, differentiation, migration, and survival of stem cells during embryogenesis, affect melanogenesis, hematopoiesis, and gametogenesis, resulting in leucistic phenotypes with severe diseases such as infertility and anemia, as well as causing perinatal death, in domestic mice (Besmer et al. 1993).

In laboratory animals, pleiotropic mutations causing leucism are often accompanied by severe diseases that seriously limit individual fitness. Since such deleterious mutations should be purged from wild populations, leucism typically observed in wild mammal species would be expected to be caused by mutations not associated with such severe diseases. However, little is known about the genes or mutations responsible for leucism in wild populations, with the exception of those on partial leucistic or diluted phenotypes, namely *SLC45A2* for white stripes in the Bengal tiger, *Panthera tigris tigris* (Xu et al. 2013), and *MC1R* for the pale yellow coat in the black bear, *U. americanus* (Ritland et al. 2001; Mills and Patterson 2009).

One critical reason why genes responsible for white hairs have not been well studied in wild populations is the impossibility of the forward genetic approach—comparisons between individuals with different phenotypes (e.g., all individuals are white in a species such as the polar bear). To understand the genetic background for white hair coloration, it would be useful to focus on new phenotypes caused by a spontaneous mutation in wild populations where all individuals display a constant coat color (e.g., white-colored mutants occurring in an agouti-colored population, and *vice versa*). If such mutants could grow into adults and reproduce in nature, they would be ideal models to identify causative mutations not associated with serious diseases.

The grey red-backed vole, *Myodes rufocanus*, is broadly distributed in the northern part of the Eurasian continent, including Hokkaido, Japan, from which the subspecies *M. rufocanus bedfordiae* is known (Nakata et al. 2015). The typical pelage color of adult voles in Hokkaido is dark brown on the back and ivory white or murky white on the belly (Nakata et al. 2015). However, there have been several reports of aberrant pelage colors, including albinism (Miyatsu et al. 1988), partial leucism (Aizawa and Makino 1938; Fujimaki 1974; Takahashi 1988; Iwasa 2004), and complete leucism (Murakawa 1988). We had the opportunity to collect a pregnant vole with an aberrant color phenotype: black eyes, localized black hairs, and white hairs on the entire body.

In this study, to clarify the genetic factors associated with the leucistic phenotype, focusing on an inbred vole pedigree exhibiting coat color variations, we performed linkage analyses to evaluate associations between the individual phenotypes and genotypes of six candidate genes: *Kit*, *Kitl*, *melanocyte-inducing transcription factor* (*Mitf*), *paired box 3* (*Pax3*), *snail family transcriptional repressor 2* (*Snai2*), and *SRY-box transcription factor 10* (*Sox10*). To remove the possibility that low genetic diversities in the inbred system may lead to false correlations between genotypes and phenotypes, we also explored allelic variations of the candidate genes in the source population where the leucistic vole was collected.

Materials and methods

Vole samples

A pregnant grey red-backed vole, *M. rufocanus bedfordiae*, was collected from a broadleaf forest with a floor covered with broad-leaf bamboo, *Sasa* sp., in Oyafuru, Hokkaido, northern Japan (43°11'N, 141°22'E), on September 18, 2013. Although adult voles commonly have an agouti-colored coat, as shown in Fig. 1a (Nakata et al. 2015), the collected female (Mrbw01) exhibited a leucistic phenotype with black eyes and white fur covering the entire body, accompanied by black hairs that typically occurred on the face, ears, dorsum, and rump (Fig. 1b).

Voles were bred to produce first- and second-generation inbred offspring, and each individual was kept until death; the age of samples ranged from 7 to 402 days. The traits described as follows are the phenotypes observed in dead individuals, however we could not determine the phenotypes in detail in some lost samples. The vole female (Mrbw01) produced six F1 offspring on October 2, 2013, comprising three agouti-colored females (Mrbw02–04) and three white-colored individuals with black hairs, including one female (Mrbw05) and two

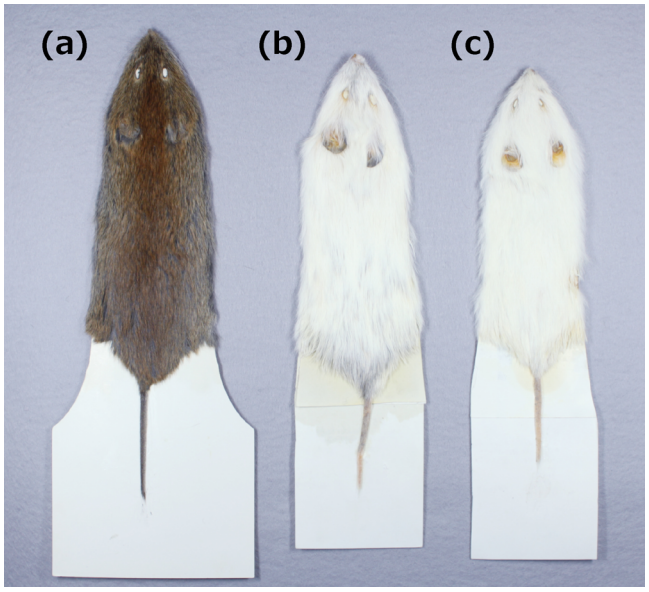

Fig. 1. Coat color variations in grey red-backed voles: (a) wild type with dark brown hair on the back and ivory or murky white on the belly (agouti); (b) leucism with black hairs (partial leucism); and (c) leucism without black hairs (complete leucism).

males (Mrbw06 and 07; Fig. 2, Supplementary Table S2). The agouti-colored F1 females (Mrbw02–04) were mated with a leucistic F1 male (Mrbw07), which yielded 35 F2 offspring (Mrbw08–42; Fig. 2, Supplementary Table S2). The F2 voles had agouti-colored coats or white coats with varying amounts of black hairs, including white-furred individuals with almost no black hairs (Fig. 1c).

We also collected 20 agouti-colored voles from the study site where the leucistic vole (Mrbw01) had been collected to explore allelic variations of the *Kit* and *Mitf* markers in the wild, which were associated with coat colors based on the linkage analyses. Because the results of the linkage analyses were based on inbred samples, which should make it easier to estimate significant associations between genotypes and phenotypes, we investigated whether the observed associations also occurred in the wild population with high allelic diversity. In this study, we treated animals following the "Guidelines for the Procedure of Obtaining Mammal Specimens" provided by the Mammal Society of Japan (https://www.mammalogy.jp/en/guideline.pdf). Vole specimens are

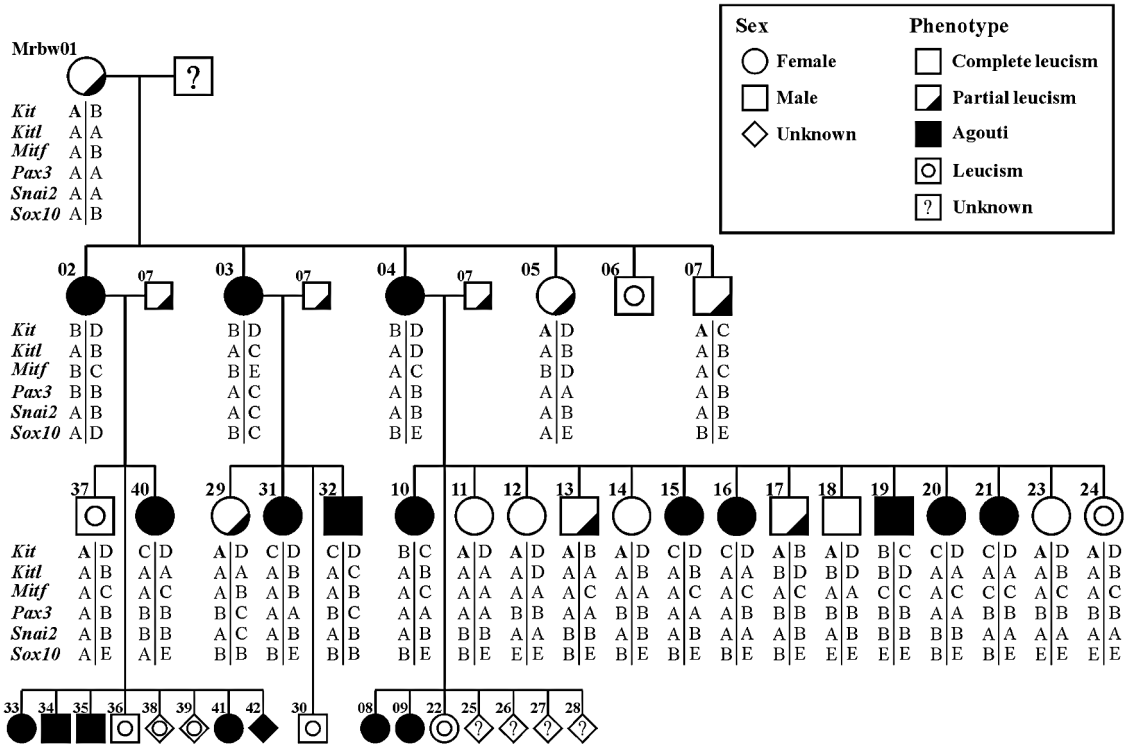

Fig. 2. Pedigree chart showing individual phenotypes of coat colors and genotypes of six gene markers: *Kit*, *Mitf*, *Kitl*, *Pax3*, *Snai2*, and *Sox10*. The Arabic numbers on each symbol identify sample names. Capital letters under symbols indicate alleles of the genetic markers. The phenotype "leucism" indicates an uncertain leucistic phenotype, for which presence or absence of black hairs could not be determined because specimens were lost (Mrbw24 and 37).

stored in the museum in the Botanic Garden of Hokkaido University.

Phenotyping

To define different leucistic phenotypes based on the presence or absence of black hairs, we quantified the area of black hairs on a white coat. The data was also used in later regression analyses to consider temporal changes in leucistic phenotypes among individuals of different ages. Using a camera (EOS Kiss X3; Canon, Tokyo, Japan) set to the f-number of 32, shutter speed of 1/32 s, and ISO of 100, we took photographs of the dorsal fur of flat skin specimens of the leucistic voles. The specimens were placed in a white box (21 cm width, 30 cm length, 21 cm height), in which the interior was adjusted to a color temperature of 5000 K using light-emitting diode strips. On the images of each specimen, we excluded yellowish areas, which were colored by subcutaneous fat, using the ImageJ 1.53e software (Schneider et al. 2012) and setting thresholds on hue (0–255), saturation (40–255), and brightness (100–255). The range was manually specified slightly within the contour of the specimen, and images were binarized using a threshold ranging from 0 to 180. The number of black and white pixels on the binarized images was counted, and the relative area of black hairs against total area was calculated. We defined partial and complete leucism from a bimodal distribution of the individual traits.

Genotyping of candidate gene markers

We investigated individual genotypes of gene markers in the 22 inbred voles, including the wild-captured F0 female, four F1 offspring, and 17 F2 offspring, as well as 20 voles from the wild. The following six genes known to be responsible for pigment losses in laboratory animals were targeted as candidate gene markers (Reissmann and Ludwig 2013): *Kit* (Besmer et al. 1993; Duttlinger et al. 1993; Yoshida et al. 2001; Hauswirth et al. 2013), including tyrosine kinase domain, in which mutations cause severe leucism (Oiso et al. 2013), *Kitl* (Besmer et al. 1993; Huang et al. 1993), *Mitf* (Moore 1995; Steingrímsson et al. 2004), *Pax3* (Tassabehji et al. 1992; Hauswirth et al. 2013), *Snai2* (Pérez-Losada et al. 2002; Sánchez-Martín et al. 2002; Cobaleda et al. 2007), and *Sox10* (Verastegui et al. 2000; Hou et al. 2006).

Genomic DNA was extracted from muscle tissues using the phenol–chloroform method (Sambrook and Russell 2001) or using the QIAamp DNA Mini Kit or QIAamp DNA Investigator Kit (Qiagen, Hilden, Germany). Oligonucleotide primers were newly designed to specifically probe complementary sequences of the target regions (Supplementary Table S1), referring to two rodent sequences from the National Center for Biotechnology Information (NCBI) database: the deer mouse, *Peromyscus maniculatus* (NCBI Accession No. GCF_000500345), and the prairie vole, *Microtus ochrogaster* (NC_022027). We amplified a portion of each marker gene by polymerase chain reaction (PCR). Each reaction was performed with the following thermal cycling profile: initial denaturation at 95°C for 10 min, followed by 35–45 cycles of denaturation at 94°C for 30 s, annealing for 30 s at 50–56°C, and elongation for 45–60 s at 72°C. Cycle numbers, temperatures, and times were adjusted to enable efficient amplification of each genetic marker. PCR mixtures (21 μL) were composed of 1 μL of genomic template DNA, 1 μL of 10 μM forward and reverse primers, 8 μL of H_2O, and 10 μL of AmpliTaq Gold 360 DNA polymerase (Applied Biosystems, Foster City, CA, USA). Cycle sequencing reactions were performed on amplified PCR products according to the protocol of the BigDye Terminator v3.1 Cycle Sequencing Kit (Applied Biosystems), and the products were directly sequenced using the ABI 3130 Automated Sequencer (Applied Biosystems). We manually aligned sequences of the genetic markers using ProSeq ver. 2.91 alignment software (Filatov 2002).

Then, we compared the *Kit* sequences determined in this study with those of the following species from the NCBI database: the golden hamster, *Mesocricetus auratus* (NCBI Accession No. XM_013121056), prairie vole, *M. ochrogaster* (XM_005359361), deer mouse, *P. maniculatus* (XM_006979722), house mouse, *Mus musculus* (XM_017320687), Norway rat, *Rattus norvegicus* (XM_006250909), domestic cat, *Felis catus* (KU351088), grey wolf, *Canis lupus* (XM_005627970), polar bear, *U. maritimus* (XM_008701524), pig, *Sus scrofa* (JQ839266), killer whale, *Orcinus orca* (XM_012532461), cattle, *Bos taurus* (XM_005207937), goat, *Capra hircus* (XM_018049156), horse, *Equus caballus* (XM_005608573), crab-eating macaque, *Macaca fascicularis* (XM_015450467), chimpanzee, *Pan troglodytes* (XM_016951725), human, *Homo sapiens* (XM_017008180), and chicken, *Gallus gallus* (NM_204361). The nucleotide positions of the *Kit* sequences of *M. rufocanus* were determined by referring to those of the murine *Kit* cDNA sequences from the NCBI nucleotide database (BC075716).

Statistical analysis

We conducted linkage analyses to evaluate the associations between coat color phenotypes and the genotypes of the six candidate genes. For several loci in which the number of single-nucleotide polymorphic sites in a single fragment was insufficient to characterize each allele (*Kit*, *Mitf*, *Snai2*, and *Sox10*), multiple regions were concatenated into a long sequence, because we assumed that no recombination likely occurred between adjacent marker regions within each locus. Based on the individual genotypes of the markers, individual alleles were inferred using the PHASE program with Bayesian statistical methods (Stephens et al. 2001). Using the program FASTLINK (Cottingham et al. 1993), we calculated the logarithm of odds (LOD) scores using the following formula:

$$\text{LOD score } (\theta) = \log_{10}(L_\theta / L_{0.5}),$$

where θ is the recombination rate between two loci and ranges from 0 to 0.5, and L_θ and $L_{0.5}$ are likelihoods that individual phenotypes can be explained by given genotype data on a pedigree under the assumptions that the two loci are linked ($0 < \theta < 0.5$) or not ($\theta = 0.5$), respectively. The LOD score is the ratio between the likelihoods under the two assumptions (linked or unlinked), indicating a magnitude of an association between genotypes and phenotypes. We applied a Bonferroni correction to define the rigorous significance threshold (Dunn 1961; Armstrong 2014). Given that we performed 12 tests in each regression analysis (six candidate genes × two kinds of inheritance mode), the significance thresholds were defined as *P*-value of 0.000083 (0.001/12), 0.00083 (0.01/12), and 0.0042 (0.05/12), equivalent to LOD scores of 4.08, 3.08, and 2.38, respectively. LOD scores were calculated at increments of 0.01 from 0 to 0.5 of the assumed recombination rates. A significantly high maximum LOD score under a low recombination rate reflects the possibility of a linkage between a marker region and a responsible region for a phenotype of interest (Morton 1955).

In the analysis of the leucistic or agouti phenotypes, we used 22 individuals from the inbred vole pedigree. We did not include the F1 female (Mrbw02) and its F2 offspring (Mrbw37 and 40) for the linkage analyses, because genetic disagreement was observed in *Pax3* genotypes: Mrbw01 was homozygous for allele A, whereas Mrbw02 was homozygous for allele B, suggesting a newly arisen mutation in the F1 female (Mrbw02). For the analysis of the presence or absence of black hairs (partial or complete leucism), we did not include individuals in which the presence or absence of black hairs could not be determined due to specimen lost (Mrbw24 and 37) and the three individuals with genetic disagreement between parents and offspring (Mrbw02, 37, and 40) were excluded from the analysis. Consequently, we included 13 individuals: 11 leucistic individuals, which is known about the presence or absence of black hairs, plus the two F1 individuals (Mrbw03 and 04) of which phenotypes were considered as unknown due to agouti phenotype. We fixed the following parameters for all analyses: the frequencies of responsible alleles for a phenotype of interest were set to 0.01, assuming that the leucistic and black hairs on the leucistic phenotypes are rare in the wild, and sex difference rates for a phenotype of interest were set to zero. We performed linkage analyses under the following two assumptions. First, we considered both the dominant and recessive inheritance modes for responsible genes due to the uncertainty of the inheritance modes. Second, we assumed multiple paternity for mating between the wild female (Mrbw01) and unknown wild males, as promiscuity is known in this species (Nakata et al. 2015); this mating pattern was supported by the fact that more than four inferred alleles were observed among F1 offspring from four genetic markers (*Kitl*, *Mitf*, *Pax3*, and *Sox10*; Fig. 2, Table 1, Supplementary Table S2).

An analysis of covariance (ANCOVA) was used to test whether the influence of age as a covariate on body length differed between different phenotypes, leucism and agouti. The body length was calculated by subtracting tail length (basal flexure to fleshy tail-tip) from total length (nose to fleshy tail-tip). We included in the analysis only voles in which precise birth and death date information was available. In addition, Mrbw23 (seven days in age; Table 1, Supplementary Table 2) was excluded as an outlier for the following reasons. First, the rate of increase in body size of *M. rufocanus* is so different in developmental stages, as rapid before 30 days in age but gradual after 30 days in age (Abe 1968); and second, the homogeneity of the rate of increase in body length between different phenotypes of leucism and agouti was testable only in the range from 32 to 402 days in age (Table 1).

We assessed whether the proportion of black hairs on a white coat increased with individual age and body length. The proportion of black hairs was calculated by the *cbind* function in R software, combining the number of black pixels to that of white pixels. We used a generalized linear model (glm) with logit link and binomial

Table 1. Characteristics of the grey red-backed voles that were obtained in a breeding experiment and from field collection

Name	Source	Coat color phenotype[a]	Prop. of black hairs (%)	Age (days)	BL (mm)	Parent[b]	Gen	Marker[c]									
								Kit		*Kitl*	*Mitf*				*Pax3*	*Snai2*	*Sox10*
								e11–e13	concat	p–i1	e1, i1	e3, i3	i9, e10	concat	i1	concat	concat
Mrbw01	wild	partial leucism	4.04	263<	127.0	–	F0	A / B	A / B	A / A	A / B	A / B	A / B	A / B	A / A	A / A	A / B
Mrbw02	breed	agouti	–	402	124.0	1 × –	F1	B / C	B / D	A / B	B / C	B / C	B / C	B / C	B / B	A / B	A / D
Mrbw03	breed	agouti	–	401	132.0	1 × –	F1	B / C	B / D	A / C	B / C	B / D	B / D	B / E	A / C	A / C	B / C
Mrbw04	breed	agouti	–	274	130.0	1 × –	F1	B / C	B / D	A / D	A / C	A / C	A / C	A / C	A / B	A / B	B / E
Mrbw05	breed	partial leucism	8.30	385	120.5	1 × –	F1	A / C	A / D	A / B	B / C	B / E	A / B	B / D	A / A	A / B	A / E
Mrbw07	breed	partial leucism	9.46	401	135.0	1 × –	F1	A / B	A / C	A / B	A / C	A / C	A / C	A / C	A / B	A / B	B / E
Mrbw10	breed	agouti	–	81	112.0	4 × 7	F2	B / B	B / C	A / B	A / C	A / C	A / C	A / C	A / A	A / B	B / E
Mrbw11	breed	complete leucism	0.96	93	117.0	4 × 7	F2	A / C	A / D	A / A	A / A	A / A	A / A	A / A	A / A	B / B	B / E
Mrbw12	breed	complete leucism	1.05	34	106.5	4 × 7	F2	A / C	A / D	A / D	A / A	A / A	A / A	A / A	B / B	A / A	E / E
Mrbw13	breed	partial leucism	4.09	34	111.5	4 × 7	F2	A / B	A / B	A / A	A / C	A / C	A / C	A / C	A / A	B / B	B / E
Mrbw14	breed	complete leucism	0.07	32	100.0	4 × 7	F2	A / C	A / D	A / B	A / A	A / A	A / A	A / A	B / B	A / B	B / E
Mrbw15	breed	agouti	–	32	103.0	4 × 7	F2	B / C	C / D	A / B	A / C	A / C	A / C	A / C	A / A	A / B	B / E
Mrbw16	breed	agouti	–	32	104.0	4 × 7	F2	B / C	C / D	A / A	A / C	A / C	A / C	A / C	A / B	A / A	B / E
Mrbw17	breed	partial leucism	6.91	32	112.0	4 × 7	F2	A / B	A / B	B / D	A / C	A / C	A / C	A / C	B / B	A / B	B / E
Mrbw18	breed	complete leucism	0.43	32	108.0	4 × 7	F2	A / C	A / D	B / D	A / A	A / A	A / A	A / A	B / B	A / B	E / E
Mrbw19	breed	agouti	–	32	109.0	4 × 7	F2	B / B	B / C	B / D	C / C	C / C	C / C	C / C	B / B	B / B	E / E
Mrbw20	breed	agouti	–	75	–	4 × 7	F2	B / C	C / D	A / A	A / C	A / C	A / C	A / C	A / A	B / B	B / E
Mrbw21	breed	agouti	–	75	–	4 × 7	F2	B / C	C / D	A / A	C / C	C / C	C / C	C / C	B / B	A / A	B / E
Mrbw23	breed	complete leucism	0.44	7	44.0	4 × 7	F2	A / C	A / D	A / B	A / C	A / C	A / C	A / C	B / B	A / A	E / E
Mrbw24	breed	leucism	–	8	–	4 × 7	F2	A / C	A / D	A / B	A / C	A / C	A / C	A / C	B / B	A / A	E / E
Mrbw29	breed	partial leucism	8.74	335	125.0	3 × 7	F2	A / C	A / D	A / A	A / B	A / B	A / B	A / B	B / C	A / C	B / B
Mrbw31	breed	agouti	–	257	115.0	3 × 7	F2	B / C	C / D	A / B	A / B	A / B	A / B	A / B	A / A	A / B	B / E
Mrbw32	breed	agouti	–	90	115.0	3 × 7	F2	B / C	C / D	A / C	A / B	A / B	A / B	A / B	B / C	A / B	B / B
Mrbw37	breed	leucism	–	–	–	2 × 7	F2	A / C	A / D	A / B	A / C	A / C	A / C	A / C	A / B	A / B	A / E
Mrbw40	breed	agouti	–	–	119.0	2 × 7	F2	B / C	C / D	A / A	A / C	A / C	A / C	A / C	B / B	B / B	A / E
KTF-114	wild	agouti	–	–	–	–	–	B / C	– / –	– / –	(D) / (E)	A / G	A / A	(J) / (M)	– / –	– / –	– / –
KTF-115	wild	agouti	–	–	–	–	–	C / E	– / –	– / –	E / E	A / G	A / A	L / M	– / –	– / –	– / –
KTF-116	wild	agouti	–	–	–	–	–	C / H	– / –	– / –	(C) / (H)	A / F	A / A	U / V	– / –	– / –	– / –
KTF-117	wild	agouti	–	–	–	–	–	C / D	– / –	– / –	E / F	A / J	A / A	L / S	– / –	– / –	– / –
KTF-118	wild	agouti	–	–	–	–	–	B / C	– / –	– / –	F / G	F / F	A / E	(Q) / (X)	– / –	– / –	– / –
KTF-119	wild	agouti	–	–	–	–	–	B / C	– / –	– / –	(F) / (J)	A / A	A / A	(O) / (AA)	– / –	– / –	– / –
KTF-120	wild	agouti	–	–	–	–	–	C / E	– / –	– / –	C / E	D / G	A / D	E / M	– / –	– / –	– / –
KTF-153	wild	agouti	–	–	–	–	–	C / E	– / –	– / –	E / G	A / G	(A) / (G)	(N) / (W)	– / –	– / –	– / –
KTF-216	wild	agouti	–	–	–	–	–	B / C	– / –	– / –	C / F	D / D	A / A	G / T	– / –	– / –	– / –
KTF-217	wild	agouti	–	–	–	–	–	B / C	– / –	– / –	C / F	D / D	A / A	G / T	– / –	– / –	– / –
KTF-218	wild	agouti	–	–	–	–	–	B / H	– / –	– / –	(C) / (H)	A / F	A / F	U / W	– / –	– / –	– / –
KTF-219	wild	agouti	–	–	–	–	–	F / F	– / –	– / –	C / C	C / C	A / C	C / F	– / –	– / –	– / –
KTF-220	wild	agouti	–	–	–	–	–	C / F	– / –	– / –	(D) / (I)	C / C	A / I	(F) / (K)	– / –	– / –	– / –
KTF-221	wild	agouti	–	–	–	–	–	C / I	– / –	– / –	C / F	(A) / (H)	A / A	(H) / (R)	– / –	– / –	– / –
KTF-222	wild	agouti	–	–	–	–	–	F / F	– / –	– / –	A / F	A / C	(A) / (H)	(O) / (Z)	– / –	– / –	– / –
KTF-223	wild	agouti	–	–	–	–	–	B / C	– / –	– / –	C / C	(D) / (I)	A / A	G / Y	– / –	– / –	– / –
KTF-224	wild	agouti	–	–	–	–	–	F / G	– / –	– / –	(G) / (I)	A / A	A / A	(I) / (V)	– / –	– / –	– / –
KTF-230	wild	agouti	–	–	–	–	–	B / C	– / –	– / –	C / C	D / D	A / A	G / G	– / –	– / –	– / –
KTF-231	wild	agouti	–	–	–	–	–	F / F	– / –	– / –	C / G	A / A	A / A	H / V	– / –	– / –	– / –
KTF-232	wild	agouti	–	–	–	–	–	B / C	– / –	– / –	C / F	C / C	A / A	F / P	– / –	– / –	– / –

Prop. of black hairs, proportion of black hairs; BL, body length; Gen, generation; [a]The phenotype "leucism" indicates an uncertain leucistic phenotype, for which the presence or absence of black hairs could not be determined because specimens were lost (Mrbw24 and 37). [b]The Arabic numbers show individual sample names. [c]p, promoter; e, exon; i, intron; concat, concatenated; letters indicate individual alleles; statistically uncertain alleles are indicated in parentheses.

distribution error. The goodness-of-fit for the glm was estimated by the index of the McFadden's pseudo R^2 (McFadden 1974). ANCOVA and glm analyses were performed using R version 3.6.1 (R Core Team 2019).

Results

Phenotyping

In a vole pedigree consisted of 26 individuals, we quantified the proportion of black hairs by the ImageJ 1.53e (Schneider et al. 2012) on the images of the 11 specimens with leucistic phenotypes (Fig. 2). Black hairs were present on the face and tips of the ears, on the back gradually increasing to the rump, and at the base of the tail (Fig. 1b). The proportion of black hairs in each individual showed a range from 0.07% to 9.46% (Table 1). The histogram showed a bimodal distribution that allowed us to define complete or partial leucism as an area of black hairs of less than about 1% (0.07–1.05%) or more than 4% (4.04–9.46%), respectively.

Genotyping of candidate gene markers

Three to five concatenated alleles, characterized by multiple single-nucleotide polymorphisms, were inferred in each of the six gene markers (Tables 1 and 2). Each nucleotide sequence is registered in the NCBI database (NCBI Accession No. LC360812–LC360882). A nonsynonymous substitution was only obtained in the *Kit* marker (Table 2). The substitution (c.1810G>A) was located in the first codon position on exon 12 of *Kit*, resulting in the replacement of glycine with arginine at amino acid position 604 (p.Gly604Arg; Fig. 3).

A pedigree chart was constructed to illustrate individual genotypes and phenotypes (Fig. 2). More than four alleles in several genetic markers (*Kitl*, *Mitf*, *Pax3*, and *Sox10*) were observed among the F1 offspring, indicating that the female (Mrbw01) had mated with multiple males in the wild (Fig. 2, Table 1, Supplementary Table S2). The individuals with the leucistic phenotype were all heterozygous for allele A with the nonsynonymous substitution (c.1810G>A) of the *Kit* marker, whereas the individuals with the agouti-colored phenotype did not have the allele. In the *Pax3* marker, we observed a genetic incongruence between a parent and its offspring: the F0 female (Mrbw01) was homozygous for allele A, whereas its daughter (Mrbw02) was inexplicably homozygous for allele B, characterized by the additional substitution c.85+270A>G in intron 1 on allele A.

Analysis of 20 agouti-colored voles (KTF-numbered samples) from Oyafuru, where the leucistic female (Mrbw01) was collected, revealed nine alleles in the *Kit* marker fragment including exon 12, and 24 alleles of the concatenated *Mitf* marker (Table 1, Supplementary Table S2). Allele A of the *Kit* marker with the nonsynonymous substitution (c.1810G>A) was not observed among the agouti-colored wild individuals (Table 1). For the *Mitf* marker, 14 alleles, including alleles C and E, observed in the inbred pedigree were significantly inferred by the PHASE program, whereas the other ten alleles were inferred with low certainty due to many single-nucleotide polymorphisms (Table 1, Supplementary Table S2).

The nonsynonymous substitution (c.1810G>A) observed in the leucistic individuals of the inbred pedigree did not exist in the database sequences of rodent species or in Carnivora, Cetartiodactyla, Perissodactyla, Primates, and Aves (Fig. 3). Furthermore, the amino

Table 2. Nucleotide substitutions in six gene markers

Gene	Observed number of alleles	Observed number of SNPs		Character of substitutions in exon	
		Intron	Exon	Site (region)	Type[a]
Kit	4	0	3	c.54T>C (exon 1)	S
				c.1800C>T (exon 12)	S
				c.1810G>A (exon 12)	N
Kitl	4	4	0	–	–
Mitf	5	18	1	c.1230G>C (exon 10)	S
Pax3	3	2	0	–	–
Snai2	3	5	0	–	–
Sox10	5	5	1	c.342A>G (exon 1)	S

[a]S, synonymous substitution; N, nonsynonymous substitution.

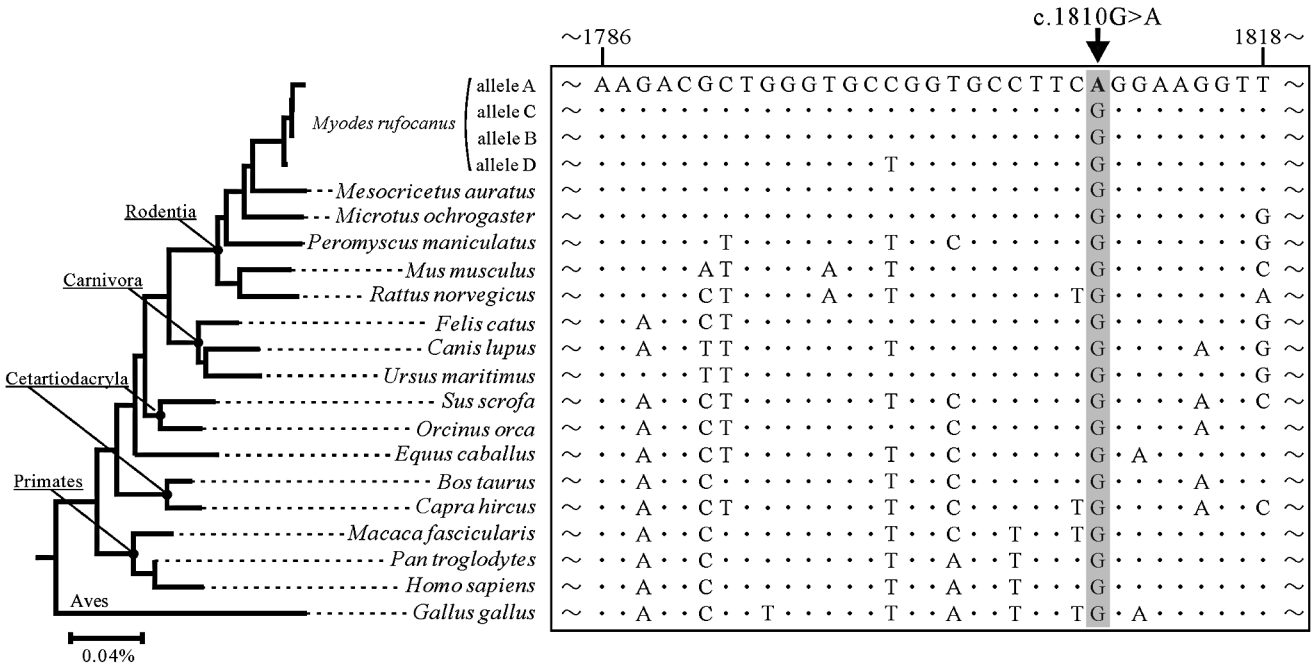

Fig. 3. A phylogenetic tree inferred from the *Kit* exon 12 region from broad taxa and their nucleotide sequences. The phylogenetic tree was constructed using the neighbor-joining method with MEGA 7 (Kumar et al. 2016).

Table 3. Maximum logarithm of odds (LOD) scores between coat color variations and genetic markers

Phenotypic variation	Gene marker	Dominant	Recessive
Leucism	*Kit*	5.42*** (θ = 0.00)	0.00
	Kitl	0.00	0.00
	Mitf	0.38 (θ = 0.25)	0.77 (θ = 0.19)
	Pax3	0.08 (θ = 0.35)	0.00
	Sox10	0.02 (θ = 0.35)	0.00
	Snai2	0.00	0.00
Sparse black hairs on the leucism	*Kit*	1.73 (θ = 0.11)	2.06 (θ = 0.00)
	Kitl	0.00	0.00
	Mitf	0.00	2.05 (θ = 0.00)
	Pax3	0.15 (θ = 0.33)	0.00
	Sox10	0.23 (θ = 0.25)	0.86 (θ = 0.27)
	Snai2	0.00	0.00

Recombination rate θ is shown only for non-zero LOD scores. ***, threshold greater than 4.08 with $P < 8.3 \times 10^{-5}$; **, greater than 3.08 with $P < 8.3 \times 10^{-4}$; *, greater than 2.38 with $P < 4.2 \times 10^{-3}$.

acid sequence from position 589 to 639 in KIT proteins was highly conserved in mammals, except for the amino acid substitution of p.Gly604Arg caused by the nonsynonymous substitution of c.1810G>A (Fig. 3).

Linkage analyses

Using 22 individuals from the inbred vole pedigree, we evaluated associations between coat color phenotypes and genotypes of each of the six candidate gene markers. Under the assumption of autosomal dominant inheritance mode for the responsible gene for the leucistic phenotype, we obtained a maximum LOD score of 5.42 under a recombination rate of zero between the *Kit* marker and the responsible genomic region for leucism (Table 3). The score was robustly higher than the Bonferroni corrected threshold for significance (LOD = 4.08, $P = 8.3 \times 10^{-5}$), equivalent to $P = 0.001$. We observed a significantly high LOD score only in the *Kit* marker, whereas the other max-

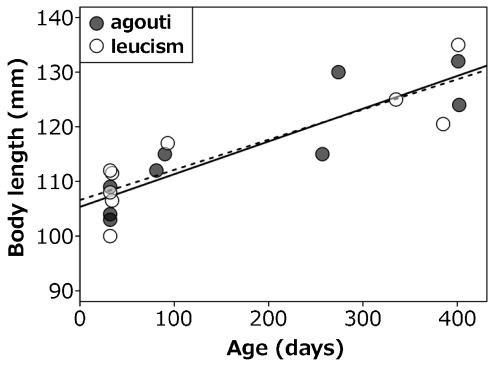

Fig. 4. Relationship between individual age and crown–rump body length in agouti and leucistic voles. Solid and dashed lines represent linear regressions in agouti and leucism, respectively.

imum LOD scores at the other gene markers were zero (*Kitl* and *Snai2*) or non-significant at high recombination rates (*Mitf*, *Pax3*, and *Sox10*; Table 3). When we assumed the autosomal recessive inheritance mode for the leucism, the maximum LOD scores were zero (*Kit*, *Kitl*, *Pax3*, *Sox10*, and *Snai2*) or non-significant with a recombination rate of 0.19 (*Mitf*; Table 3).

In linkage analyses for the 11 individuals, which is known about the presence or absence of black hairs and the two F1 individuals (Mrbw03 and 04) with assumed unknown phenotype, we obtained no significant maximum LOD scores between any genetic marker and the phenotypes under the assumption of autosomal dominant inheritance mode for the black hairs (Table 3). Assuming the autosomal recessive inheritance mode for the phenotype, we obtained marginal maximum LOD scores of 2.06 and 2.05 at a recombination rate of zero for the *Kit* and *Mitf* markers, respectively (Table 3); meanwhile, the other markers had maximum LOD scores of zero (*Kitl*, *Pax3*, and *Snai2*) or non-significant values at a recombination rate of 0.27 (*Sox10*; Table 3).

Growth-associated coat color changes

In the ANCOVA model, the covariate of age was the strongest term ($F_{1, 14} = 47.62$, $P < 0.0001$), whereas the phenotypes ($F_{1, 14} = 0.035$, $P = 0.85$) and the interaction term between age and phenotypes ($F_{1, 14} = 0.079$, $P = 0.78$) was not significant (Fig. 4). These results indicated that age affected body length positively, and that body length and increase rate of body length did not differ between different phenotypes (Fig. 4).

We detected significantly positive relationships between the relative area of black hairs in the leucistic phenotypes and age (estimate ± *SE* = $3.99 \times 10^{-3} \pm 6.51 \times 10^{-6}$, $z = 612.0$, $P < 0.0001$; Fig. 5a) or body length (estimate ± *SE* = $5.16 \times 10^{-2} \pm 9.47 \times 10^{-5}$, $z = 545.0$, $P < 0.0001$; Fig. 5b). The proportion of variance in the dependent variable explained by age and body length were 42% ($R^2 = 0.42$) and 52% (McFadden's pseudo $R^2 = 0.52$), respectively. Almost all individuals younger than 100 days old were complete leucism with 0.07% to 1.05% of black hair, with the exception of the two individuals, Mrbw13 (34 days old) and Mrbw17 (32 days old), in which proportion of black hairs were 4.09 and 6.91%, respectively. On the other hands, individuals over 100 days old all exhibited partial leucism with the proportion of black hairs ranging from 4.04% to 9.46% (Fig. 5a, Table 1). Individuals less than 110 mm in body length exhibited the complete leucistic phenotype with the proportion of black hairs ranging from 0.07% to 1.05%. Individuals from 110 to 120.5 mm showed a drastic increase in the proportion of black hairs up to 8.30%. Individuals over 120.5 mm all exhibited the partial leucistic phenotype, with the proportion of black hairs ranging from 4.04% to 9.46% (Fig. 5b, Table 1).

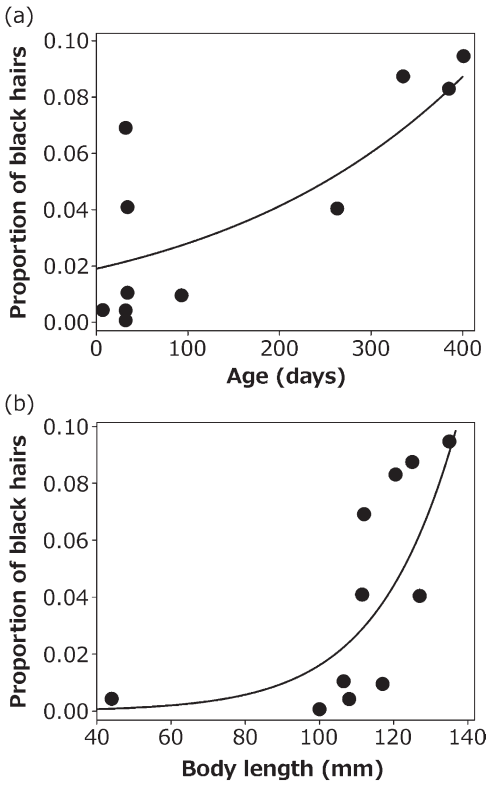

Fig. 5. Relationship (a) between individual age and the relative area of black hairs in leucistic voles, and (b) between individual crown–rump body length and the relative area of black hairs in leucistic voles.

Discussion

Genetic cause of the leucistic phenotype

The proximate cause underlying leucistic phenotypes observed in wild populations of mammalian species has been poorly understood. Here, focusing on a leucistic phenotype observed in the grey red-backed vole, *M. rufocanus*, we revealed an association between the leucistic phenotype and the *Kit* allele in a dominant inheritance manner (Table 3). Leucistic voles were all heterozygous for allele A containing a nonsynonymous substitution in exon 12 (c.1810G>A), which changed an amino acid from glycine to arginine at amino acid position 604 (Fig. 2, Tables 1 and 2). In 20 agouti-colored voles collected from the wild, the nonsynonymous substitution characterizing allele A of *Kit* was not detected (Table 1), indicating that the mutation may not be prevalent in the wild population and is newly arisen.

Kit encodes a transmembrane receptor tyrosine kinase that is activated by dimerization upon binding of its ligand, KITL proteins. During early embryogenesis in mice, *Kitl* is expressed in the branchial arch mesenchyme of the head and the dorsal aspect of the dermatome in the trunk and the tail (Wehrle-Haller 2003). It has been postulated that KITL proteins have a chemotactic function in attracting or guiding melanocyte precursors, melanoblasts, which express the *Kit* gene, resulting in the migration of melanoblasts onto the dorsolateral migration path between the ectoderm and the dorsal surface of the somite (Wehrle-Haller 2003). Therefore, mutations in *Kit* affect KIT kinase activity, inhibit melanocyte deposition, and cause pigment loss (Nocka et al. 1990; Marklund et al. 1998; Haase et al. 2007). Of the missense mutations of murine *Kit* listed in the Mouse Genome Informatics (MGI) database (Eppig et al. 2005), mutation sites are concentrated in the domains of tyrosine kinase 1 (10/28 sites) and 2 (11/28 sites), and furthermore, missense mutations in the tyrosine kinase domain have been shown to cause severe leucism (Oiso et al. 2013). For example, white spots were observed on mice with heterozygous $Kit^{w\text{-}v}$ carrying the missense mutation c.2007C>T located in the tyrosine kinase 1 domain (Nocka et al. 1990).

It is noteworthy that the nonsynonymous substitution (c.1810G>A, p.Gly604Arg) observed in this study is located in tyrosine kinase domain 1 of the *Kit* gene, and the glycine residue at position 604 is the last one in a highly conserved ATP binding motif, Gly-X-Gly-X-X-Gly motif (Kamps et al. 1984; Yarden et al. 1987) in wide array of mammalian taxa, as well as a bird species. This indicates that the missense mutation in the conserved motif may prevent the binding of ATP, the phosphate transfer reaction of KIT proteins and subsequent signaling cascades. In particular, missense mutations in the tyrosine kinase domain should result in a more severe phenotype because they inhibit autophosphorylation during heterodimer formation of normal and abnormal proteins, and thus individuals heterozygous for the mutations have only 25% of functional activity of KIT dimer (Oiso et al. 2013). The missense mutation in this study should disturb the proper development of melanocytes, resulting in unpigmented hairs via a deficiency of melanocytes in the skin of leucistic individuals.

Because *Kit* exhibits pleiotropic effects on melanogenesis, gametogenesis, and hematopoiesis, mutations in the gene cause leucism and also impaired fertility and anemia (Besmer et al. 1993). However, the leucistic voles with the nonsynonymous substitution (c.1810G>A) reproduced normally, and the increase rate of body length did not differ between leucism and agouti according to our ANCOVA (Fig. 4; $F_{1, 14} = 0.079$, $P = 0.78$). These results indicate that the substitution affects only melanogenesis, or at least would not impact germ cell lines and individual growth. Although the causative genes have not yet been identified in the wild mammals because of the difficulty of the forward genetic approach, this study suggests that leucism-related genes widely known to also trigger other diseases in laboratory animals can be responsible for leucistic phenotypes in wild mammal species showing no maladaptive diseases. On the other hand, human Gly601Arg, the homologous mutation to the Gly604Arg in this study, cause a distinct phenotype: a large depigmented skin patch on forehead and multiple large areas of depigmented skin scattered over body accompanied by a left congenital hand abnormality of three digits with complete cutaneous syndactyly and an underdeveloped left forearm compared to the right (Syrris et al. 2000), implying that the consequence of the homologous mutation differed depending on organisms. In addition, an absence of melanocytes may impair other important functions, such as ultraviolet protection (Reissmann and Ludwig 2013).

Additional reverse genetic studies using the CRISPR/Cas9-mediated knock-out method (Cong et al. 2013) are necessary to evaluate the impacts of this nonsynonymous substitution on organisms. As a supplementary experiment for this study, we tried to make the knock-out mouse with the targeted point mutation in *Kit* (c.1810G >A; see Supplemental Experiment Procedure). Through

the experiment, we failed to introduce the targeted point mutation (c.1810G>A), but obtained a *Kit* knock-out mouse with an oligonucleotide insertion by the CRISPR/Cas9-mediated knock-out method for agouti-colored background ICR × C57/B6 mice. The knock-out mouse exhibited pigment losses on the belly and on the tips of the forefoot (Supplementary Fig. S1). In the mouse, the 13-nucleotide insertion (5'-AGATGTTTAGCAA-3') replaced the original six-nucleotide sites from 1807 to 1812 (5'-TTCGGG-3') in exon 12 of the *Kit* locus, leading to a frameshift mutation with multiple translational stop codons; the first one of them provided translation termination at the amino acid residue 610, equivalent to the nucleotide position 1830. Haploinsufficiency characterized by truncated proteins due to a frameshift mutation should preserve approximately 50% of the KIT function, leading to a mild phenotype such as the partial leucism on the belly and forefoot rather than the white fur covering the entire body (Oiso et al. 2013).

In several leucistic voles, black hairs were partially visible on the face, ears, back, and rump (Fig. 1b). During early embryogenesis in mice, a proportion of melanoblasts in the craniofacial and caudal regions have already acquired c-kit independence (Yoshida et al. 1996). Thus, even in mice with unfunctional KIT proteins, which is required for melanoblast migration and survival, there should still be melanocytes not to migrate and survive in the regions. In fact, a phenotype obtained in mice by injection of KIT inhibitors during the melanoblast migration stage (Yoshida et al. 1996) was similar to the phenotype of leucism with small portion of black hairs seen in this study. The black hairs observed on the face and rump observed in the present study would be the result of remaining KIT-independent melanocytes producing melanins.

Kit and *Mitf* were each slightly associated with the expression of black hairs on the leucistic phenotype in an autosomal recessive inheritance manner (Table 3). However, neither gene was the responsible locus, because there were discordances between marker genotypes and coat color phenotypes. For instance, individuals exhibiting the partial leucistic phenotype (Mrbw05 and 29) had alleles A and D of the *Kit* marker, whereas other individuals with the complete leucistic phenotype (Mrbw11, 12, 14, 18, and 23) also had the same alleles (Fig. 2, Table 1). Similarly, for the *Mitf* marker, one individual with the complete leucistic phenotype (Mrbw23) had alleles A and C, whereas other individuals with the same phenotype (Mrbw11, 12, 14, and 18) had only allele A. Such genotype-phenotype discordances are unexpected under a study design using a family with several generations that would have had little opportunity for recombination.

Growth-associated coat color changes

The proportion of black hairs on the leucistic phenotype significantly increased as age and body length increased (Fig. 5). All individuals with a body length less than 110 mm displayed complete leucism, whereas most individuals over 110 mm had partial leucism, except one individual (Mrbw11). In captivity, coat color is known to change with growth in grey red-backed voles from a dark hairs all over the body to a reddish-brown coat color once they are 110–120 mm in body length around 50 days old (Abe 1968; Ota 1984). The black hairs on the leucism phenotype observed in this study may be the result of pigment production and accumulation in the few remaining melanocytes due to the nonsynonymous *Kit* mutation, resulting in a growth-associated change in coat color. Although we could not investigate a change in the coat color in agouti phenotype that could be compared to the one in leucism, these phenomena appear to show distinct reaction norms between agouti and leucistic phenotypes, raising cautions to conduct studies on hair color without considering growth.

Although we could not conclude from the two possibilities for the proximate mechanisms underlying the darkening in the leucistic voles: the result of a simple accumulation of homeostatically produced melanin or growth-associated change in gene expression of melanin production. If the former is true, the degree of darkening should be strongly related to individual age. However, the variation was explained better by body length (McFadden's pseudo $R^2 = 0.52$) than age ($R^2 = 0.42$; Fig. 5). In other words, the latter hypothesis that some gene expression may promote melanin synthesis as body length increased was more likely. It is noteworthy that recent studies have shown that in $Oca2^{p\text{-}cas}/Oca2^{p\text{-}cas}$ mice with a C57BL/6J genetic background, an unknown recessive gene may cause progressive darkening of the eye and coat colors with aging (Ishikawa et al. 2015).

To our knowledge, this is the first study to suggest that a leucistic phenotype observed in a wild mammal population is caused by genes responsible for a severe disease-associated leucistic phenotype known in laboratory animals. Our results showed that the leucism observed in grey red-backed voles was associated with the nonsynonymous substitution in the *Kit* exon 12. The observation of growth-associated change in coat

color on leucistic voles implied cautions to consider growth-dependencies in coat color in future studies.

Supplementary data

Supplementary data are available at *Mammal Study* online.
Supplementary Fig. S1. A *Kit*-knock out mouse by CRISPR/Cas9 system. The pigment losses on the belly and tips of the forefoot are indicated by left and right arrows, respectively.
Supplementary Table S1. Oligonucleotide primers used in this study.
Supplementary Table S2. Characteristics of the grey red-backed voles that were obtained in a breeding experiment and from field collection.
Supplemental Experimental Procedure

Acknowledgments: We thank members of the Laboratory of Ecology and Genetics, Graduate School of Environmental Earth Science, Hokkaido University, for their helpful discussion. This study was conducted with the support of a grant-in-aid for Scientific Research (C) to HS (No. 15K07177) from the Japan Society for the Promotion of Science.

References

Abe, H. 1968. Growth and development in two forms of *Clethrionomys*. 1. External characters, body weight, sexual maturity and behaviour. Bulletin of the Hokkaido Forest Experimental Station (Bibai) 6: 69–89 (in Japanese with English summary).

Aizawa, T. and Makino, S. 1938. On a vole, *Clethrionomys rufocanus bedfordiae* with an aberrant coat colour. Transactions of the Sapporo Natural History Society 15: 187–190.

Armstrong, R. A. 2014. When to use the Bonferroni correction. Ophthalmic and Physiological Optics 34: 502–508.

Baxter, L. L., Watkins-Chow, D. E., Pavan, W. J. and Loftus, S. K. 2019. A curated gene list for expanding the horizons of pigmentation biology. Pigment Cell and Melanoma Research 32: 348–358.

Besmer, P., Manova, K., Duttlinger, R., Huang, E. J., Packer, A., Gyssler, C. and Bachvarova, R. F. 1993. The *kit*-ligand (steel factor) and its receptor c-*kit*/*W*: pleiotropic roles in gametogenesis and melanogenesis. Development 119 (Supplement): 125–137.

Best, T. L. and Henry, T. H. 1994. *Lepus arcticus*. Mammalian Species: 1–9.

Caro, T. 2005. The adaptive significance of coloration in mammals. Bioscience 55: 125–136.

Caro, T. and Mallarino, R. 2020. Coloration in mammals. Trends in Ecology and Evolution 35: 357–366.

Cieslak, M., Reissmann, M., Hofreiter, M. and Ludwig, A. 2011. Colours of domestication. Biological Reviews 86: 885–899.

Cobaleda, C., Pérez-Caro, M., Vicente-Dueñas, C. and Sánchez-García, I. 2007. Function of the zinc-finger transcription factor *SNAI2* in cancer and development. Annual Review of Genetics 41: 41–61.

Cong, L., Ran, F. A., Cox, D., Lin, S., Barretto, R., Habib, N., Hsu, P. D., Wu, X., Jiang, W., Marraffini, L. A., et al. 2013. Multiplex genome engineering using CRISPR/Cas systems. Science 339: 819–823.

Cott, H. B. 1940. Adaptive Coloration in Animals. Methuen & Co. Ltd., London, 540 pp.

Cottingham, R. W. Jr., Idury, R. M. and Schäffer, A. A. 1993. Faster sequential genetic linkage computations. American Journal of Human Genetics 53: 252–263.

Dunn, O. J. 1961. Multiple comparisons among means. Journal of the American Statistical Association 56: 52–64.

Duttlinger, R., Manova, K., Chu, T. Y., Gyssler, C., Zelenetz, A. D., Bachvarova, R. F. and Besmer, P. 1993. *W-sash* affects positive and negative elements controlling c-*kit* expression: ectopic c-*kit* expression at sites of kit-ligand expression affects melanogenesis. Development 118: 705–717.

Eppig, J. T., Bult, C. J., Kadin, J. A., Richardson, J. E., Blake, J. A., Anagnostopoulos, A., Baldarelli, R. M., Baya, M., Beal, J. S., Bello, S. M., et al. 2005. The Mouse Genome Database (MGD): from genes to mice—a community resource for mouse biology. Nucleic Acids Research 33: D471-5. DOI: 10.1093/nar/gki113.

Filatov, D. A. 2002. proseq: a software for preparation and evolutionary analysis of DNA sequence data sets. Molecular Ecology Notes 2: 621–624.

Fox, H. M. and Vevers, G. 1960. The Nature of Animal Colours. Macmillan, New York, 246 pp.

Fujimaki, Y. 1974. An albino red-backed vole, *Clethrionomys rufocanus bedfordiae*, from Hokkaido. Journal of the Mammalogical Society of Japan 5: 194.

Haase, B., Brooks, S. A., Schlumbaum, A., Azor, P. J., Bailey, E., Alaeddine, F., Mevissen, M., Burger, D., Poncet, P., Rieder, S., et al. 2007. Allelic heterogeneity at the equine *KIT* locus in dominant white (*W*) horses. PLOS Genetics 3: e195. DOI: 10.1371/journal.pgen.0030195.

Hauswirth, R., Jude, R., Haase, B., Bellone, R. R., Archer, S., Holl, H., Brooks, S. A., Tozaki, T., Penedo, M. C. T., Rieder, S., et al. 2013. Novel variants in the *KIT* and *PAX3* genes in horses with white-spotted coat colour phenotypes. Animal Genetics 44: 763–765.

Hou, L., Arnheiter, H. and Pavan, W. J. 2006. Interspecies difference in the regulation of melanocyte development by SOX10 and MITF. Proceedings of the National Academy of Sciences of the United States of America 103: 9081–9085.

Huang, E. J., Manova, K., Packer, A. I., Sanchez, S., Bachvarova, R. F. and Besmer, P. 1993. The murine steel panda mutation affects kit ligand expression and growth of early ovarian follicles. Developmental Biology 157: 100–109.

Ishikawa, A., Sugiyama, M., Hondo, E., Kinoshita, K. and Yamagishi, Y. 2015. Development of a novel pink-eyed dilution mouse model showing progressive darkening of the eyes and coat hair with aging. Experimental Animals 64: 207–220.

Iwasa, M. A. 2004. A note on aberrant pelage colors in a wild population of the gray red-backed vole *Clethrionomys rufocanus bedfordiae* in Hokkaido. Mammal Study 29: 93–95.

Kamler, J. F. 2008. Ear flashing behaviour of cape hares (*Lepus capensis*) in South Africa. African Journal of Ecology 46: 443–444.

Kamler, J. F. and Ballard, W. B. 2006. Ear flashing behavior of black-tailed jackrabbits (*Lepus californicus*). American Midland Naturalist 155: 402–403.

Kamps, M. P., Taylor, S. S. and Sefton, B. M. 1984. Direct evidence that oncogenic tyrosine kinases and cyclic AMP-dependent protein kinase have homologous ATP-binding sites. Nature 310:

589–592.
Kumar, S., Stecher, G. and Tamura, K. 2016. MEGA7: molecular evolutionary genetics analysis version 7.0 for bigger datasets. Molecular Biology and Evolution 33: 1870–1874.
Little, C. C. 1915. The inheritance of black-eyed white spotting in mice. American Naturalist 49: 727–740.
Marklund, S., Kijas, J., Rodriguez-Martinez, H., Rönnstrand, L., Funa, K., Moller, M., Lange, D., Edfors-Lilja, I. and Andersson, L. 1998. Molecular basis for the dominant white phenotype in the domestic pig. Genome Research 8: 826–833.
McFadden, D. 1974. Conditional logit analysis of qualitative choice behavior. In (Zarembka, P., ed.) Frontiers in Econometrics, pp. 105–142. Academic Press, New York.
Mills, M. G. and Patterson, L. B. 2009. Not just black and white: pigment pattern development and evolution in vertebrates. Seminars in Cell and Developmental Biology 20: 72–81.
Miyatsu, T., Konno, M. and Nitta, S. 1988. An albino red-backed vole, *Clethrionomys rufocanus bedfordiae*. Shinrin Hogo (Forest Protection) 196: 47 (in Japanese).
Moore, K. J. 1995. Insight into the *microphthalmia* gene. Trends in Genetics 11: 442–448.
Morton, N. E. 1955. Sequential tests for the detection of linkage. American Journal of Human Genetics 7: 277–318.
Motohashi, H., Hozawa, K., Oshima, T., Takeuchi, T. and Takasaka, T. 1994. Dysgenesis of melanocytes and cochlear dysfunction in mutant microphthalmia (*mi*) mice. Hearing Research 80: 10–20.
Murakawa, M. 1988. A capturing record of a white colored *Clethrionomys rufocanus bedfordiae*. Shinrin Hogo (Forest Protection) 207: 40 (in Japanese).
Nakata, K., Saitoh, T. and Iwasa, M. A. 2015. *Myodes rufocanus* (Sundevall, 1846). In (Ohdachi, S. D., Ishibashi, Y., Iwasa, M. A., Fukui, D. and Saitoh, T., eds.) The Wild Mammals of Japan, Second edition, pp. 150–153. Shoukadoh, Kyoto.
Nocka, K., Tan, J. C., Chiu, E., Chu, T. Y., Ray, P., Traktman, P. and Besmer, P. 1990. Molecular bases of dominant negative and loss of function mutations at the murine c-*kit*/white spotting locus: W^{37}, W^{v}, W^{41} and *W*. EMBO Journal 9: 1805–1813.
Oiso, N., Fukai, K., Kawada, A. and Suzuki, T. 2013. Piebaldism. Journal of Dermatology 40: 330–335.
Ota, K. 1984. Study on Wild Murid Rodents in Hokkaido. Hokkaido University Press, Sapporo, 420 pp. (in Japanese).
Pérez-Losada, J., Sánchez-Martín, M., Rodríguez-García, A., Sánchez, M. L., Orfao, A., Flores, T. and Sánchez-García, I. 2002. Zinc-finger transcription factor Slug contributes to the function of the stem cell factor c-kit signaling pathway. Blood 100: 1274–1286.
R Core Team. 2019. R: A Language and Environment for Statistical Computing. Foundation for Statistical Computing, Vienna, Austria. Available at https://www.r-project.org/ (Accessed 3 September 2019).
Reissmann, M. and Ludwig, A. 2013. Pleiotropic effects of coat colour-associated mutations in humans, mice and other mammals. Seminars in Cell and Developmental Biology 24: 576–586.
Ritland, K., Newton, C. and Marshall, H. D. 2001. Inheritance and population structure of the white-phased "Kermode" black bear. Current Biology 11: 1468–1472.
Sambrook, J. and Russell, D. W. 2001. Molecular Cloning: A Laboratory Manual, Third edition. Cold Spring Harbour Laboratory Press, New York, 2344 pp.
Sánchez-Martín, M., Rodríguez-García, A., Pérez-Losada, J., Sagrera, A., Read, A. P. and Sánchez-García, I. 2002. *SLUG* (*SNAI2*) deletions in patients with Waardenburg disease. Human Molecular Genetics 11: 3231–3236.
Schneider, C. A., Rasband, W. S. and Eliceiri, K. W. 2012. NIH Image to ImageJ: 25 years of image analysis. Nature Methods 9: 671–675.
Shibuya, H., Watanabe, R., Maeno, A., Ichimura, K., Tamura, M., Wakana, S., Shiroishi, T., Ohba, K., Takeda, K., Tomita, H., et al. 2018. Melanocytes contribute to the vasculature of the choroid. Genes and Genetic Systems 93: 51–58.
Steingrímsson, E., Copeland, N. G. and Jenkins, N. A. 2004. Melanocytes and the *microphthalmia* transcription factor network. Annual Review of Genetics 38: 365–411.
Stephens, M., Smith, N. J. and Donnelly, P. 2001. A new statistical method for haplotype reconstruction from population data. American Journal of Human Genetics 68: 978–989.
Syrris, P., Malik, N. M., Murday, V. A., Patton, M. A., Carter, N. D., Hughes, H. E. and Metcalfe, K. 2000. Three novel mutations of the proto-oncogene *KIT* cause human piebaldism. American Journal of Medical Genetics 95: 79–81.
Takahashi, K. 1988. Capturing examples of white-colored individuals of *Sorex unguiculatus* and *Clethrionomys rufocanus bedfordiae* in Hokkaido. Shinrin Hogo (Forest Protection) 203: 6 (in Japanese).
Tassabehji, M., Read, A. P., Newton, V. E., Harris, R., Balling, R., Gruss, P. and Strachan, T. 1992. Waardenburg's syndrome patients have mutations in the human homologue of the *Pax-3* paired box gene. Nature 355: 635–636.
van Grouw, H. 2006. Not every white bird is an albino: sense and nonsense about colour aberrations in birds. Dutch Birding 28: 79–89.
van Grouw, H. 2013. What colour is that bird. British Birds 106: 17–29.
Verastegui, C., Bille, K., Ortonne, J. P. and Ballotti, R. 2000. Regulation of the microphthalmia-associated transcription factor gene by the Waardenburg syndrome type 4 gene, *SOX10*. Journal of Biological Chemistry 275: 30757–30760.
Wallace, A. R. 1877. The colors of animals and plants. American Naturalist 11: 713–728.
Wehrle-Haller, B. 2003. The role of Kit-ligand in melanocyte development and epidermal homeostasis. Pigment Cell Research 16: 287–296.
Xu, X., Dong, G. X., Hu, X. S., Miao, L., Zhang, X. L., Zhang, D. L., Yang, H. D., Zhang, T. Y., Zou, Z. T., Zhang, T. T., et al. 2013. The genetic basis of white tigers. Current Biology 23: 1031–1035.
Yarden, Y., Kuang, W. J., Yang-Feng, T., Coussens, L., Munemitsu, S., Dull, T. J., Chen, E., Schlessinger, J., Francke, U. and Ullrich, A. 1987. Human proto-oncogene c-*kit*: a new cell surface receptor tyrosine kinase for an unidentified ligand. EMBO Journal 6: 3341–3351.
Yoshida, H., Grimm, T., Nishimura, E. K., Nishioka, E., Nishikawa, S. I. and Kunisada, T. 2001. Melanocyte migration and survival controlled by SCF/c-kit expression. Journal of Investigative Dermatology Symposium Proceedings 6: 1–5.
Yoshida, H., Kunisada, T., Kusakabe, M., Nishikawa, S. and Nishikawa, S. I. 1996. Distinct stages of melanocyte differentiation revealed by anlaysis of nonuniform pigmentation patterns. Development 122: 1207–1214.
Zimova, M., Hackländer, K., Good, J. M., Melo-Ferreira, J., Alves, P. C. and Mills, L. S. 2018. Function and underlying mechanisms of seasonal colour moulting in mammals and birds: what keeps them changing in a warming world? Biological Reviews 93: 1478–1498.

Received 17 January 2022. Accepted 22 June 2022.
Published online 16 September 2022.
Editor was Kai He.